Angioscopy: Direct visualization of chronic venous occlusion, May-Thurner syndrome, and other applications in phlebology

Mina Kang, BMedSc,[a] Claudia Hurwitz, MBBS,[a] Tom Exner, PhD,[b] Anes Yang, MD, BMed, MPH,[c,d] David Connor, PhD,[a,d] *and* Kurosh Parsi, MBBS, FACD, FACP, MSc, PhD,[a,c,d] *Sydney, New South Wales, Australia*

ABSTRACT

Background: Angioscopy has been widely used in the diagnosis and management of vascular disorders and in particular in coronary artery disease. However, few applications have been developed in the diagnosis or management of venous disease.

Methods: Endovenous angioscopy was performed to explore applications of this modality in phlebology. Procedures were performed in a sterile setting. Access was obtained by ultrasound guidance and a 9F introducer sheath. An 8.5F videoscope was used to visualize target veins. Continuous saline irrigation was used to displace blood and to clear the visual field.

Results: Fifteen procedures were performed. We describe diagnostic or interventional applications of endovenous angioscopy that include diagnosis and characterization of chronic venous occlusion, deployment of venous stents, angioscopy-guided thrombectomy, foam sclerotherapy, and endovenous laser ablation. Chronic venous occlusion was observed to be fibrotic rather than thrombotic.

Conclusions: Endoscopic imaging of the venous system has great potential to improve access and to guide endovenous interventions. Chronic venous occlusion in post-thrombotic syndrome is a fibrotic process, and chronic venous fibrosis is a better description of the type of occlusion and should replace chronic venous thrombosis. (J Vasc Surg: Venous and Lym Dis 2019;7:870-81.)

Keywords: Angioscopy; May-Thurner syndrome; Chronic venous thrombosis; Post-thrombotic syndrome; Endovenous laser ablation

Diagnostic investigation of the venous system is restricted to imaging modalities that do not directly visualize the tissue. Currently, the main imaging modalities of the venous system are duplex ultrasound (DUS), venography in combination with computed tomography or magnetic resonance imaging, and intravascular ultrasound (IVUS).

Endoscopic imaging is a widely used modality in different fields of medicine, including arthroscopy, laparoscopy, gastrointestinal tract endoscopy, wireless video camera endoscopy, coronary angioscopy, and laryngoscopy. Direct visualization provides more information on luminal morphologic and pathologic features than other imaging modalities that require image interpretation. The major advantage of endoscopic imaging is its diagnostic real-time direct view of target tissue and, if necessary, its ability to facilitate intervention in real time. The use of endoscopic imaging in endovascular surgery has been limited by the difficulty of displacing blood in target vessels.[1] A transparent fluid such as saline, heparinized saline, dextran, or Ringer solution is used to displace blood and to obtain a clear field of vision. When this is the only maneuver employed to displace blood, the technique is called nonobstructive angioscopy. The deployment of balloons in addition to the fluid irrigation to achieve a clear field of vision is called obstructive angioscopy.[2]

Given the technical complexities, vascular applications of endoscopic imaging have been limited. Japanese researchers have the greatest experience, having described multiple applications in coronary artery disease[3-7] and aortic disease.[2] We could identify only a handful of reports[8-14] in the English literature from Western countries published in the late 1980s and early 1990s describing the use of angioscopy in a venous setting.

From the Faculty of Medicine, University of New South Wales[a]; the Haematex Research Pty Ltd[b]; and the Department of Dermatology,[c] and Dermatology, Phlebology and Fluid Mechanics Research Laboratory, St. Vincent's Centre for Applied Medical Research,[d] St. Vincent's Hospital.

Author conflict of interest: none.

Additional material for this article may be found online at www.jvsvenous.org.

Correspondence: A/Prof. Kurosh Parsi, MBBS, FACD, FACP, MSc, PhD, Dermatology, Phlebology and Fluid Mechanics Research Laboratory, St. Vincent's Centre for Applied Medical Research, Level 8, Lowy-Packer Bldg, 405 Liverpool St, Darlinghurst, New South Wales 2010, Australia (e-mail: kurosh.parsi@svha.org.au).

The editors and reviewers of this article have no relevant financial relationships to disclose per the Journal policy that requires reviewers to decline review of any manuscript for which they may have a conflict of interest.

2213-333X

https://doi.org/10.1016/j.jvsv.2019.05.008

Here, we present our 4-year experience in applying this modality to a range of venous conditions. We also present our technique to improve and to simplify endoscopic imaging in the hope of reviving its use in endovascular surgery.

METHODS

Ethics. The project was approved by St. Vincent's Human Research Ethics Committee, and informed written consent was obtained from all patients on all occasions. Patients undergoing endovenous laser ablation (EVLA) and ultrasound-guided foam sclerotherapy were consented for intraoperative visualization of the effects of laser and foam on the vessel wall and the potential requirement of multiple procedures in case of failure of the initial treatment.

Materials. The angioscope used was Flex-XC (Karl Storz, Tuttlingen, Germany), a 70-cm-long, 8.5F flexible videoscope providing a 1920 × 1080p high-definition image. Image and data capture was managed by an interface system (AIDA Compact Neo v3.2; Karl Storz). Fluoroscopy was performed using Veradius Unity mobile C-arm (Philips, Amsterdam, The Netherlands). Ultrasound imaging was provided by Aplio 500 Platinum Series and 18-7 MHz linear transducer (Canon, Tokyo, Japan). Other materials included an introducer set (Prelude SNAP; Merit Medical Systems, Malvern, Pa), 1500-nm endovenous laser system (INTERmedic, Barcelona, Spain), tumescent infusion pump (Klein Infiltration Pump; HK Surgical, San Clemente, Calif), and sodium tetradecyl sulfate (STS; Fibrovein; STD Pharmaceuticals Ltd, Hereford, United Kingdom).

Setup. All procedures were performed in a hybrid theater, an operating room equipped with advanced medical imaging including a fixed C-arm enabling minimally invasive surgery. All patients received mild sedation and were discharged on the same day of the procedure.

Patients were initially positioned supine on the operating table to gain access. For imaging of the great saphenous vein (GSV), the lower limbs were elevated to 15 to 30 degrees to assist with narrowing of the lumen to clear the intravascular blood, hence improving the visual field.

For visualizing the suprainguinal and abdominal veins, the legs were lowered to 15 to 30 degrees below the level of the pelvis. The trunk was also lowered to 15 to 30 degrees below the pelvic level, and the operating table was tilted to the left by 15 degrees to facilitate venous drainage into the heart (Fig 1).

Access. The lower extremity was prepared and draped with a sterile technique. Access was selected according to the target structure. When the target was the deep veins of the pelvis, the common femoral vein (CFV) was accessed at the inguinal crease; but when the target was the GSV, this vein was accessed at the knee level using a 9F Seldinger introducer under ultrasound guidance.

ARTICLE HIGHLIGHTS

- **Type of Research:** Single-center, retrospective study with review of the literature
- **Key Findings:** Endovenous angioscopy performed on 15 patients demonstrated potential applications in phlebology, including diagnosis and characterization of chronic venous occlusion, deployment of venous stents, angioscopy-guided thrombectomy, foam sclerotherapy, and endovenous laser ablation.
- **Take Home Message:** Endoscopic imaging of the venous system has great potential to improve access and to guide endovenous interventions.

Irrigation. The angioscope had two ports. The first port was closed with an endoscopic seal and reserved for instrumentation. The second port was connected to an intravenous giving set with 250 mL of normal saline (NS) running on free flow. The fluid bag was elevated to 2 m, which generated a constant pressure gradient to maintain the irrigation and hence did not require the use of a pressure cuff around the bag. NS was delivered through the coaxial irrigation channel to prime the scope. The fluid was then clamped and remained clamped until the scope entered the vein.

Whereas we relied on the flow to be generated by gravity, the flow rate could be further reduced manually by using the giving set's roller clamp. At the outset, we trialed the use of an irrigation pump to deliver the fluid, but this was counterproductive in clearing the visual field because of high pressures and the subsequent turbulence generated by the pump. We also trialed manually compressing the bag to increase the pressure, but this also created turbulence in the visual field.

Angioscopic technique. The angioscope was inserted into the introducer and the NS was unclamped. Free flow of NS displaced intravenous blood, clearing the visual field. The saline flow rate was controlled at an absolute minimum that would achieve the desired effect of clearing the visual field. The rate of the infusion was not kept at a constant rate and was adjusted as needed. On average, the saline flow rate was 10 mL/min to a maximum of 750 mL of saline for a 60-minute procedure. Care was taken to avoid the entry of bubbles into the target vessel.

The angioscope was then advanced to the region of interest. Its location in the leg could be traced by the transcutaneously visible light source but not when it entered the pelvis. The scope could be steered by a single-lever control handle that achieves up to 270-degree dual deflection. Careful handling of the scope was important to maintain a clear visual field as rapid movements steered blood and obstructed the view.

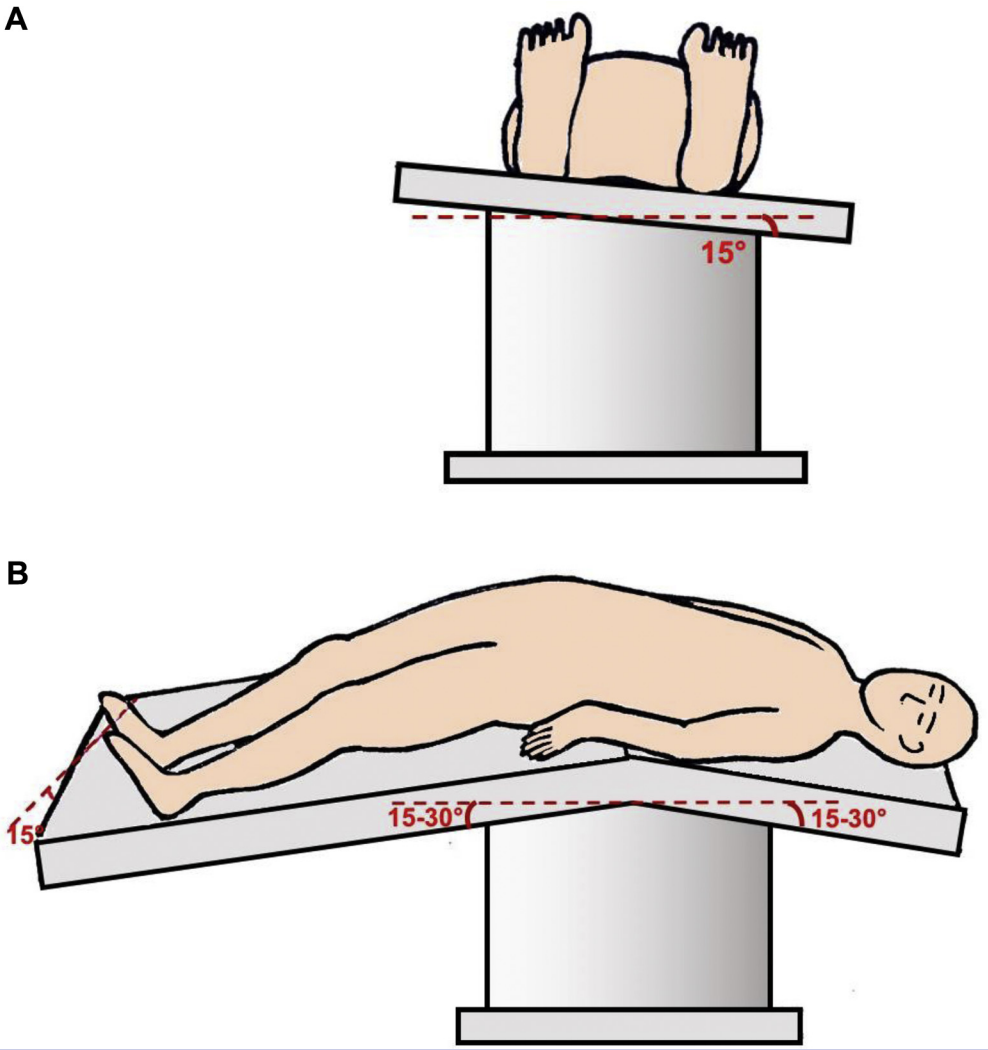

Fig 1. Schematic diagram of patient positioning (Parsi-Kang position). This position was designed to enhance venous drainage and hence to improve angioscopic visualization of abdominal and pelvic veins. **A,** Transverse view from the foot of the bed. **B,** Lateral view.

Imaging was obtained through the AIDA system and displayed on the monitors. Intervention could be administered at this point, with the first port providing a 3.6F working channel for the passage of guidewires, laser fibers, embolic agents, or suction catheters if required.

EVLA was performed as previously described.[15,16] The laser tip was maintained at about 5 to 10 mm beyond the head of the scope to avoid damage to the lens. Saline irrigation was maintained. Foam was prepared using a modified Tessari method.[17]

At the end of the procedure, the scope was retracted and the introducer was removed. The wound site was closed with sterile strips not requiring sutures.

RESULTS

Fifteen diagnostic or interventional angioscopic procedures were performed and followed up in a 4-year period (2014-2018). Clear field of view was ultimately obtained in all procedures. Our technique evolved over time, and longer duration of clear field of vision was obtained in the later procedures. There were no complications other than minor bruising at the entry point. Angioscopy was employed in the following applications.

General diagnostic applications. Angioscopy was used as an adjunct to other diagnostic modalities, including DUS and venography, when morphologic or anatomic identification (eg, existence and size of venous valves) was required. We found angioscopy useful in assisting with identification of normal anatomy (Video 1, online only).

Chronic CFV occlusion. An 83-year-old woman presented with left-sided "varicose veins" affecting her left upper thigh and extending to the lower abdomen (Fig 2, *A*). On examination, she had transpubic dilated protruding veins that extended to the left inguinal crease and left side of the abdomen. May-Thurner syndrome

was suspected. DUS demonstrated wall thickening and thrombosis extending proximally from the CFV (Fig 2, *B*). Venography demonstrated chronic occlusion of the left CFV with collateral filling of the right iliac venous system and inferior vena cava (Fig 2, *C*). The tortuous superficial veins were identified to be abdominal collaterals bypassing the occlusion. Angioscopy was performed to confirm outflow obstruction and further identify and define the nature of the occlusion. Access was obtained at the femoral vein in the thigh. There was no evidence of an acute, fresh soft thrombus. Chronic fibrosis of the CFV (chronic venous fibrosis) was observed on angioscopy (Fig 2, *D*; Video 2, online only).

May-Thurner syndrome and venous stent. A 66-year-old man was under our care with a left-sided recurrent ulceration of the medial ankle (Fig 3, *A*). His medical history was relevant for post-thrombotic syndrome, presenting with deep vein incompetence and occlusion on a background of heterozygous factor V Leiden mutation. He was anticoagulated with rivaroxaban. DUS demonstrated chronic partial occlusion of the left femoral vein (Fig 3, *B*). May-Thurner syndrome was suspected and confirmed on venography. Narrowing of the iliofemoral segment was identified. We referred him to a colleague, and a venous stent was deployed. Postoperative angioscopy (Fig 3, *C*; Video 3, online only) demonstrated patency of the segment but ongoing narrowing despite the deployment of the stent. The ulcer has reduced in size but is yet to heal at the time of this submission.

Identification of valves in truncular venous malformation. A 21-year-old man presented with deep and superficial vein incompetence of lower limb veins secondary to a congenital truncular venous malformation. His main complaint was ankle swelling. On examination, the affected leg was shorter by 1 cm compared with the contralateral limb. There was a prominent left

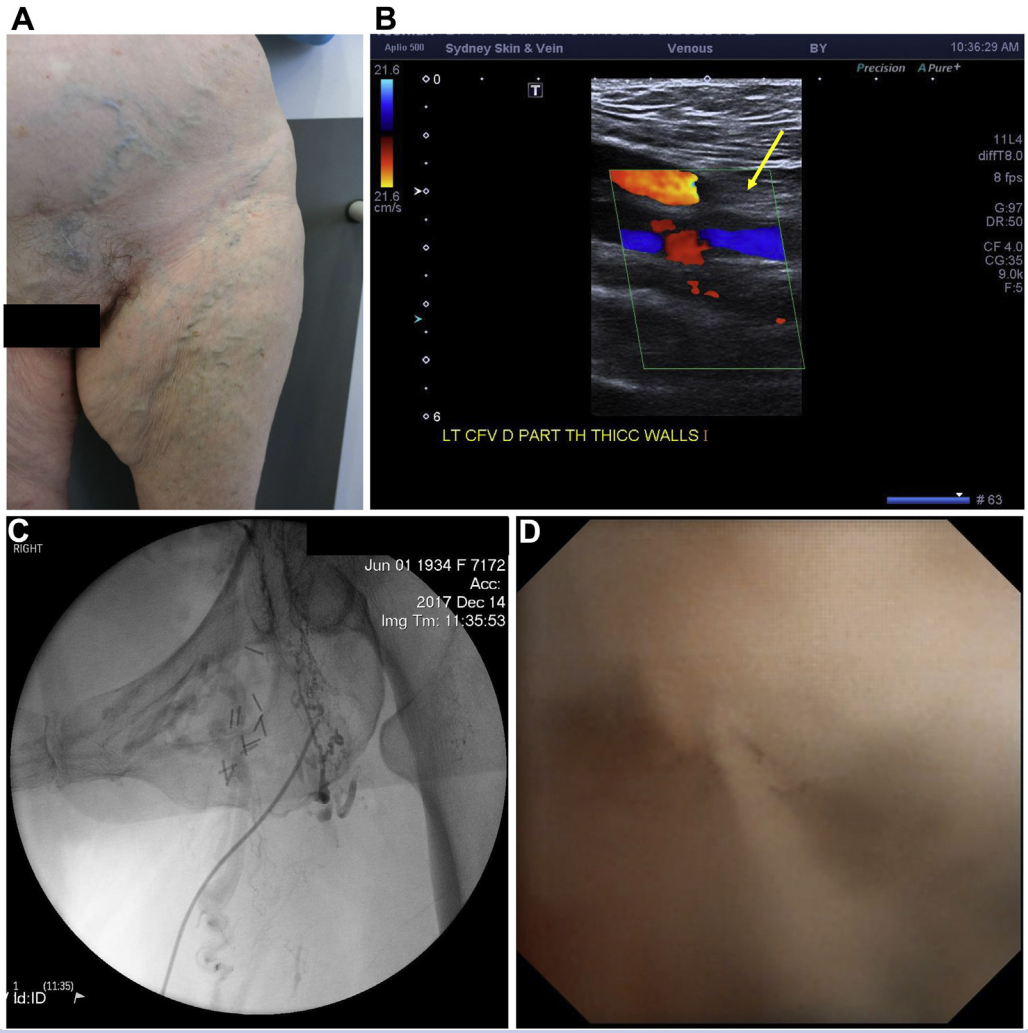

Fig 2. Chronic common femoral vein (*CFV*) occlusion. **A,** Transpubic collateral veins. **B,** Duplex ultrasound (DUS) image demonstrating left CFV wall thickening and chronic occlusion as indicated by the *arrow*. **C,** Venography of the left common femoral system. **D,** Angioscopy image visualizing chronic occlusion due to chronic venous fibrosis.

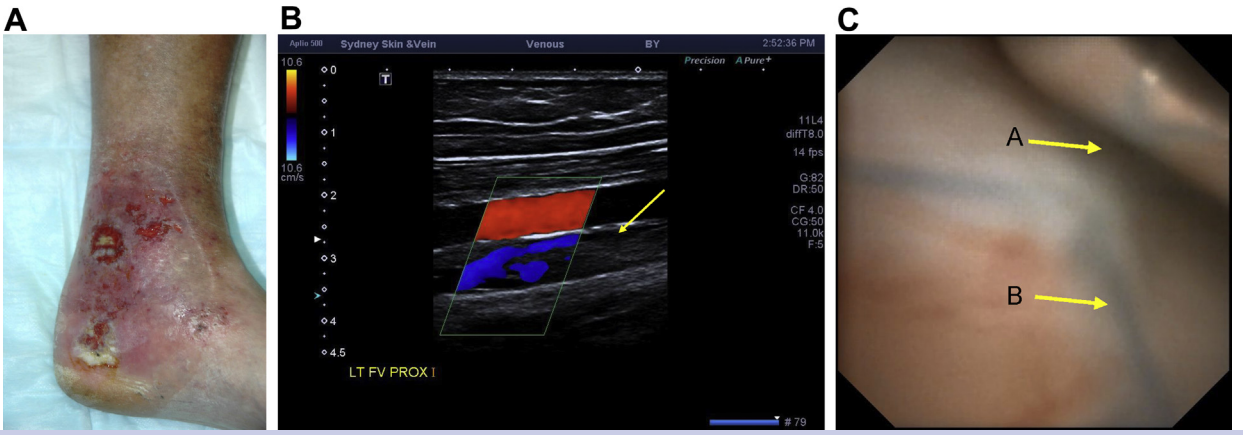

Fig 3. May-Thurner syndrome and venous stent. **A,** Recalcitrant ulceration of the left medial ankle area. **B,** Duplex ultrasound (DUS) image demonstrating chronic partial occlusion of the left femoral vein, as indicated by the *arrow*. **C,** Angioscopic visualization of stent patency in the left iliofemoral segment. *A*, Narrowed but patent lumen; *B*, stent.

anterolateral vein of the thigh. DUS showed reflux in the superficial and deep venous systems. Servelle-Martorell syndrome was diagnosed. Given the congenital nature of the condition, we wanted to exclude valvular agenesis or hypoplasia. On ultrasound examination, valves could not be discerned. We proceeded with angioscopy to look for valves and to assess the size and number of valves in the target vessel to exclude valvular agenesis or hypoplasia. Angioscopy demonstrated bicuspid hypoplastic valves with transparent walls (Fig 4; Video 4, online only) that compared with normal valves appeared smaller, and although the two leaflets came together, they were unable to completely approximate on a Valsalva maneuver. We used angioscopy to visualize venous valves not observed on B-mode ultrasound and believe this is the role of the angioscopic technique in this setting. Angioscopy cannot reliably assess for competence, given the patient's supine position and its qualitative nature. DUS remains the "gold standard" for assessment of reflux.

Angioscopy-guided EVLA. A 35-year-old man presented with massively gross and dilated lower limb varicose veins (Fig 5, *A*). The right GSV measured 8.8 mm in diameter in the upper thigh; the left GSV measured 10.7 mm (Fig 5, *B*). We treated the right leg first. He consented to angioscopy-guided EVLA using a 1500-nm laser. The procedure was performed with a constant flow of NS irrigation. The laser functioned well despite the lack of blood in the target vessel. Visualization demonstrated formation of smoke and bubbles after activation of the laser (Fig 5, *C*; Video 5, *A* and *B*, online only). Charring and substantial edema of the inner wall of the target vein were observed. After completion of the procedure, the lasered segment was revisualized, and substantial wall carbonization secondary to the heat damage was observed (Fig 5, *C*; Video 5, *C*, online only). The recovery was uneventful. On 1-week follow-up examination, despite the large size of the veins, the GSV trunk and most calf tributaries were fibrotically occluded on ultrasound evaluation as evident from the echogenic appearance of the occlusion. He required one more session of EVLA to treat the small saphenous vein and two sessions of ultrasound-guided foam sclerotherapy to treat smaller tributaries. We repeated the same protocol to treat this patient's left leg. This treatment protocol was repeated for eight other patients who also underwent angioscopy-guided EVLA. Similar observations were made in every case, with nearly complete fibrosclerosis of the treated veins on follow-up ultrasound examination. The treated veins were completely occluded at 1-week, 6-week, and 12-month follow-up (Fig 5, *D*).

Intravascular behavior of foam. The intravascular behavior of sclerosant foam was observed using angioscopy; 3 mL of STS 1.5% foam was injected through the working channel of the scope, and foam behavior was observed. Saline irrigation was maintained through the second port of the scope during the procedure. Microbubbles coalesced and rose to the top wall of the target vein (Fig 6, *A*; Video 6, *A*, online only). Larger bubbles were formed in time (Fig 6, *B*; Video 6, *A*, online only). Lone bubbles adhered to the vein wall (Fig 6, *C*; Video 6, *B*, online only), and groups of bubbles adhered to the outer surface of sclerothrombus (Fig 6, *D-F*; Video 6, *A*, online only). In time, we observed the thrombus losing its red cell component and changing from a fresh red color to a pale white (Fig 6, *G* and *H*; Video 6, *A*, online only). After about 10 minutes of observation, the endothelium of the vessel wall appeared to be peeling off (Fig 6, *I*; Video 6, *A*, online only).

Anatomic and hemodynamic observations. The saphenous vein appeared to have a fluffy cotton-like intimal surface along its trunk (Fig 7, *A*; Video 7, *A*,

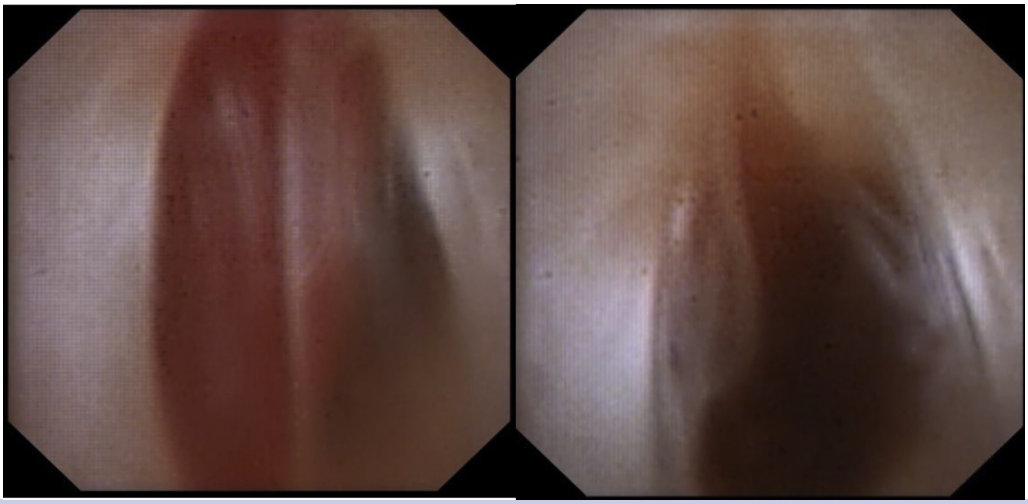

Fig 4. Identification of bicuspid valves in truncular venous malformation. Angioscopic visualization of hypoplastic valves.

online only). By contrast, the deep veins appeared to have a more robust architecture with a less cotton-like intima (Fig 7, *B*; Video 7, *B*, online only).

The vasa vasorum was observed on the luminal surface of deep veins (Fig 7, *C*; Video 7, *B*, online only) but not on the intimal layer of the GSV trunk. As expected, venous valves were bicuspid. Cusps had a central transparent surface but appeared denser closer to the attachment to the wall. The valve leaflets completely approximated and parachuted against blood flow on Valsalva maneuver (Fig 7, *D* and *E*; Video 7, *C*, online only).

In a vein filled with saline, blood preferentially traveled at the center of the lumen. Laminar flow was observed turning into a spiral flow pattern (Fig 7, *F* and *G*; Video 7, *D*, online only). This was still true when there was a large volume of blood, with blood taking a central position and saline flowing peripherally (Fig 7, *H*; Video 7, *D*, online only).

Flow of blood from tributaries of the GSV into the saphenous trunk appeared to have a phasic pattern (Fig 7, *I*; Video 7, *E*, online only).

DISCUSSION

In this study, we used angioscopy to confirm the diagnosis and management of two patients with a deep vein disease, one with CFV occlusion and one with May-Thurner syndrome. We found this tool to be extremely useful, given that in the first patient, we established complete obstruction of the femoral segment; and in the second patient, we could visually confirm the positioning of the venous stent. Endovenous angioscopy not only confirmed the findings of standard venous imaging techniques but provided the additional benefit of delineating real-time intraluminal details while providing access for interventions. Angioscopy enabled us to demonstrate that the chronic venous obstruction of the femoral vein was a fibrotic occlusion rather than a thrombotic one. Histologic and ultrasound reports by Comerota et al,[18] Labropoulos et al,[19] and others have previously suggested that chronic venous thrombosis is indeed an endovenous fibrotic process rather than a thrombotic occlusion. In case two, DUS identified the presence of occlusion through demonstration of wall thickening. Angioscopy was performed to further delineate the nature of the occlusion as either a thrombotic occlusion or a fibrotic occlusion. In addition, angioscopy demonstrated complete occlusion and absence of a lumen that could potentially allow stent placement or an intervention to achieve recanalization.

We used postoperative angioscopy to confirm the position of a venous stent placed by another physician. Currently, stent placement requires preimaging with venography or IVUS and then subsequent fluoroscopy-guided stent placement, followed by further fluoroscopy to confirm the position and patency of the stent.[20] Angioscopy allows the visualization of stent placement and intraluminal patency. This does not preclude the use of venography during stent placement but may be used as a better alternative to IVUS. Venography is essential in ensuring the most appropriate positioning of the stent to avoid kinking, fractures, and other complications, such as stent thrombosis. The immediate post-stent venogram demonstrated patency of the stent. This was in contrast to our angioscopic observation, which showed the lumen to be patent but narrowed, most likely because of compression by the inguinal ligament and the initial positioning of the stent.

Our patients treated with angioscopic EVLA had a painless recovery period. On follow-up, the results appeared impressive in terms of the nature of occlusion after the procedure, with the occlusion appearing fibrotic (echogenic on ultrasound) as against thrombotic (anechoic

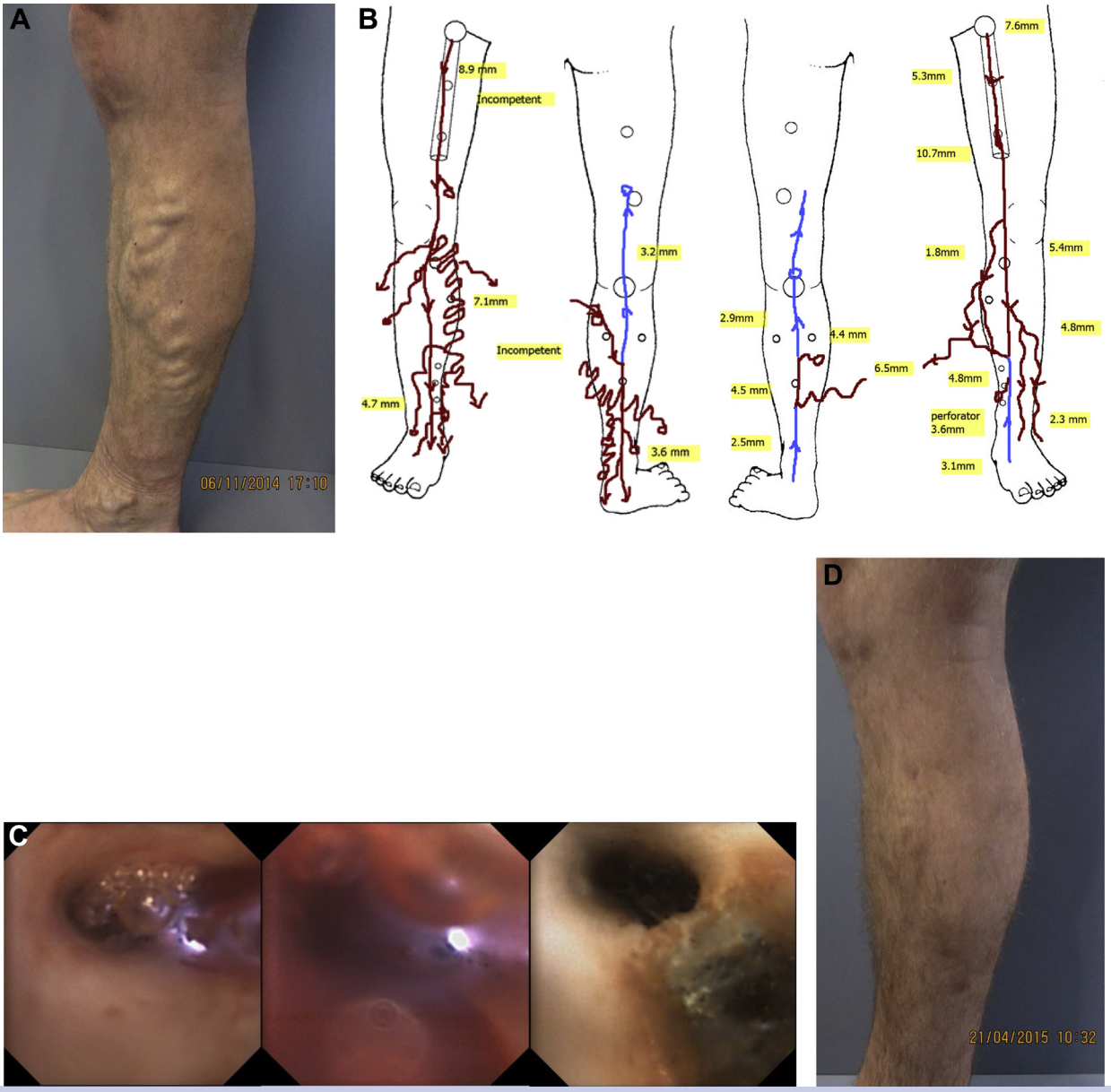

Fig 5. Angioscopy-guided endovenous laser ablation (EVLA). **A,** Before treatment: massively dilated lower limb calf varicosities in a 35-year old man. **B,** Venous mapping of lower limb superficial veins; *red* denotes incompetence, whereas *blue* means competent antegrade flow. The *numbers* indicate diameters. **C,** Angioscopic visualization of EVLA. *Left*, Bubble formation on laser activation. *Middle*, Smoke generation on laser activation. *Right*, Wall carbonization and edema on revisualization after completion of the procedure. **D,** After treatment: complete resolution of lower limb varicose veins.

on ultrasound). Our first patient, who had extremely large veins, required only two procedures to ablate the great and small saphenous systems. We believe this impressive result was due to the displacement of blood by saline used for irrigation. This improved outcome is possibly due to two processes.[21-23] First, the lack of blood would ensure a nonthrombotic occlusion, resulting in a more direct fibrotic process. In addition, and in the case of foam sclerosants, displacement of blood by intravascular saline significantly enhances the effectiveness of foam sclerosants. This is due to the prevention of deactivation of foam sclerosants by blood components, in particular erythrocyte membranes and albumin.[21-23] Our current findings support our previous in vitro and in vivo observations that the luminal content plays an important role in achieving optimal closure, supporting the concept of empty vein technique as the ideal approach.

This pilot study allowed us to understand the applications of this potentially useful technology in endovenous interventions. Although our experience is limited, our initial observations have allowed us to make modifications to procedures that we routinely perform, such as

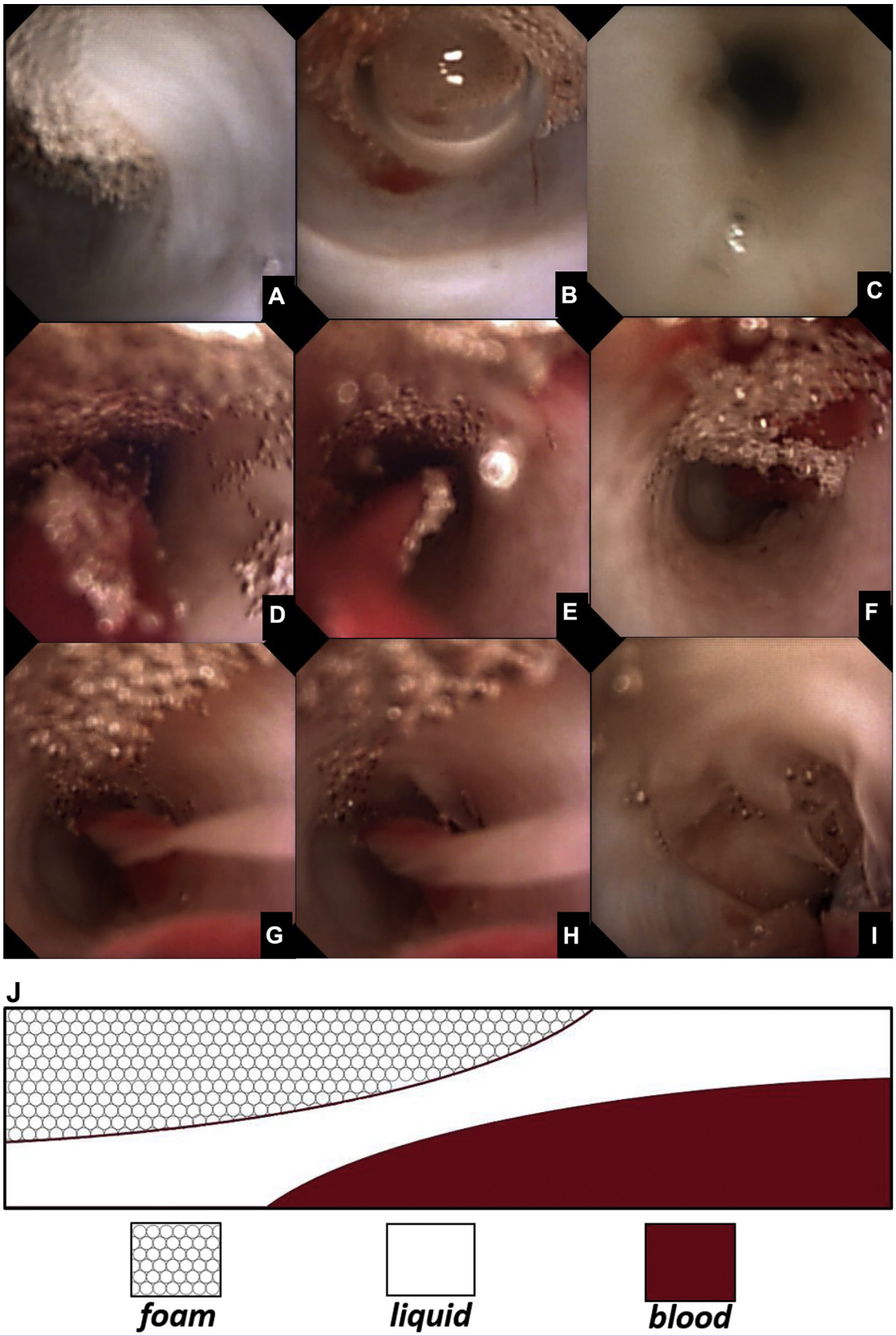

Fig 6. Intravascular behavior of foam. **A,** Angioscopic visualization of microbubbles at top wall. **B,** Angioscopic visualization of large bubble formation. **C,** Angioscopic visualization of lone bubble on the vein wall. **D-F,** Angioscopic visualization of foam bubbles adhering to sclerothrombus. **G** and **H,** Angioscopic visualization of sclerothrombus losing its red cell component to change from a fresh red color to a pale white over time. **I,** Angioscopic visualization of peeling endothelium. **J,** Three layers form when foam is injected into the target vessel. Foam ascends to the top wall and forms the top layer, liquid sclerosant forms the second layer, and blood forms the bottom layer.

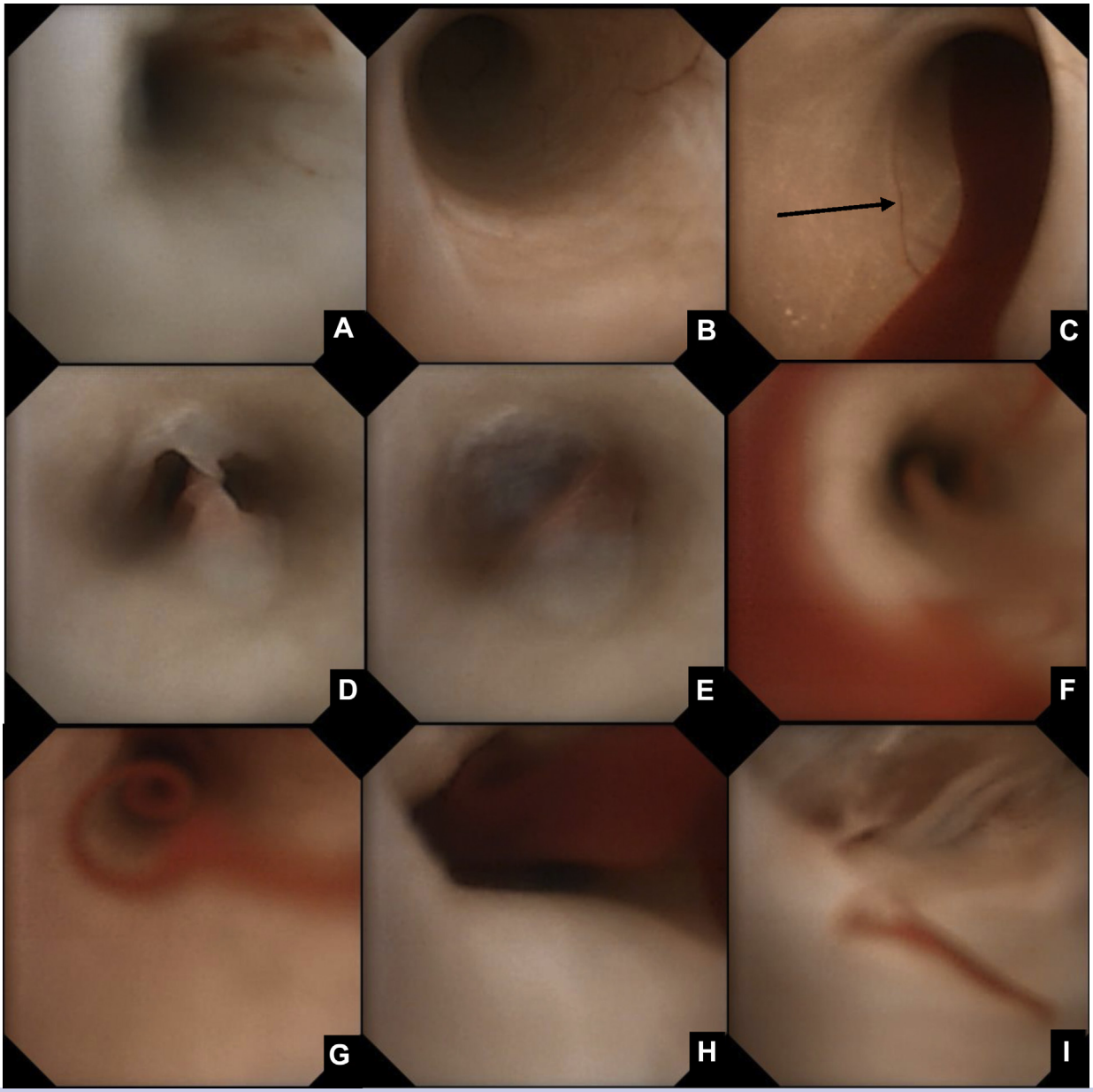

Fig 7. Anatomic and hemodynamic observations. **A,** Angioscopic visualization of great saphenous vein (GSV) cotton-like intima. **B,** Angioscopic visualization of saphenofemoral junction demonstrating a more rigid architecture compared with the GSV **(A). C,** Angioscopic visualization of vasa vasorum (*arrow*). **D,** Angioscopic visualization of bicuspid valve open. **E,** Angioscopic visualization of bicuspid valve closed. **F** and **G,** Angioscopic visualization of laminar spiral flow. **H,** Angioscopic visualization of central blood and peripheral saline flow. **I,** Angioscopic visualization of phasic side tributary flow.

the utility of saline flush in EVLA and ultrasound-guided sclerotherapy, which improved the outcome and, in our limited experience with angioscopy, expedited the process. Future studies are required to validate these observations.

We observed other interesting phenomena while performing angioscopy-guided procedures. During the EVLA procedure, some patients reported a burning smell and a metallic taste in the mouth within seconds of the commencement of the laser procedure. It has previously been concluded that heat from the laser causes carbonization of blood and surrounding tissue.[24] We observed smoke generated after commencement of the laser procedure (Video 5, *B*, online only) and believe the exhalation of this smoke is responsible for the unpleasant taste and smell. We were also able to confirm the carbonization process by directly visualizing the inner aspect of the treated veins (Video 5, *C*, online only). We used a 1500-nm laser, and this wavelength, compared with the 810 nm and 980 nm, is meant to generate less carbonization. In addition, bubbles were observed on angioscopy (Video 5, *A*, online only). These

bubbles generate the ring-down artifact observed during concurrent ultrasound.

We made another intriguing observation that we could advance back to the saphenofemoral junction after completion of the laser procedure, visualizing the damaged wall and charring of the inner lumen of the saphenous vein. The fact that the scope was effortlessly passed back up the vein with a patent lumen implies that it did not interfere with occlusion of the vein, and in fact the patient had an outstanding outcome. Our ability to pass the scope up the saphenous vein may have been facilitated by the constant irrigation with NS. This observation implies that despite popular belief, although transmural damage is obtained immediately with the activation of the laser, long-term occlusion possibly occurs during the ensuing days and is not an immediate process.

The use of angioscopy allowed us to monitor the intravascular behavior of the sclerosant foam. As previously reported by this group, foam ascends to the top wall of the target vessel and three layers are formed—foam bubbles at the top wall, a middle layer of liquid sclerosant, and a lower layer of blood[25] (Fig 6, *J*). The differentiation is due to differences in fluid density, with foam being the lightest and blood the heaviest.[26]

We observed coalescence of the foam bubbles and formation of larger bubbles, confirming our in vitro studies.[26,27] In addition, we observed the affinity of bubbles for the vein wall and surface of fresh thrombus. These observations were better appreciated on real-time imaging reproducible in videos demonstrating bubble coalescence, endothelial peeling, and attachment of the sclerosants to the thrombus (Video 6, *A*, online only). The affinity of sclerosant foam for the venous intima is not surprising, but the affinity of sclerosant foam for the thrombus was a novel observation. In this study, we used STS, which is an anionic detergent. Studies by Exner et al[28] suggested that fibrin polymers may carry a more positive charge than the precursor fibrinogen. This may explain our observation of affinity of anionic STS foam for the surface of the thrombus. In addition, this observation may be explained by the protective or stabilizing effect of the fibrin polymers on bubbles in general. A fibrin network provides a lattice for disbursement of bubbles. This property was used to manufacture fibrin foams, developed in 1949 as a topical hemostatic agent.[29] Comparative studies using polidocanol, a nonionic detergent, are required to further elucidate the possible role of the molecular charge and the role of the fibrin polymer in explaining these observations. We observed the sclerothrombus to undergo a color change from red to pale pink in a number of minutes, most likely due to the sclerosant's effect of lysing the red blood cells within the sclerothrombus.

Anatomy of the venous system is currently visualized with imaging modalities that produce a picture requiring qualitative interpretation rather than by direct images of the vessels. Angioscopy allowed direct visualization and interrogation of venous disease. We were able to identify hypoplastic valves as the pathophysiologic cause for deep vein insufficiency in our patient. Given the small size and thin tissue of valve cusps, visualization with ultrasound may be difficult and will heavily depend on the ultrasound presets, frequency of the probe, angle of insonation, compounding, and dynamic settings used. In addition, the sonographers need to be skillful in being able to visualize the venous valves and to assess the normality of size, shape, and function of each valve. Angioscopy allows direct visualization of the valve cusps and does not require any specific setting applied for the imaging. We compared the intimal surface of the GSV in midthigh with the saphenofemoral junction and observed its lumen to appear morphologically less solid; we described this surface as fluffy, whereas the saphenofemoral lumen appeared more robust. These observations were morphologic but repeatable, and the same pattern was observed in all saphenous veins examined.

Currently, if information additional to that provided by DUS is required, venography or IVUS is the next step. Venography is used to detect obstruction or thrombosis of occluded deep veins, such as the iliofemoral vein. Alternatively, computed tomography venography and magnetic resonance venography produce images of the designated area, depicting the veins and surrounding structures. However, neither of these can conclusively demonstrate obstruction of the affected vein and the nature of the obstruction. In addition, venography cannot delineate the detailed vein wall or intraluminal changes, such as webs, trabeculae, or other signs of recanalization impairing vein function.[30] An increasingly popular imaging modality is IVUS, which is able to show findings that are not visible on venographic results, including intraluminal detail such as webs, axial collateral formation, and external compression of venous lumen.[31] However, IVUS has multiple limitations, such as initial setup cost, cost of the disposable catheters, lack of availability, service and support in certain countries, lack of reimbursement from health funds in most countries, and requirement of extensive training of end users. In comparing IVUS with angioscopy, IVUS effectively generates computer-processed reconstituted graphics requiring interpretation, whereas angioscopy provides real-time, high-resolution images of the actual target tissues. Although other modalities provide indirect imaging that requires interpretation, direct imaging provides superior understanding of the surgical field and allows live visualization of the endovenous procedure, which provides confirmation of having achieved the end point of the procedure. In addition, the angioscope is sterilizable and reusable, and the initial setup cost is nowhere close to that of IVUS. There are no disposable items, and the operative time is comparable to that of IVUS. Angioscopy is, however, limited by its inability to

visualize external structures or transmural disease.[11] Remuneration and insurance rebates vary from country to country. There is currently no Medicare rebate for use of IVUS in Australia, whereas angioscopy is covered by Medicare and insurance companies, which allows compensation of the additional operative times and operating room staff.

In this study, we performed foam sclerotherapy and EVLA under direct angioscopic guidance. We are planning to perform angioscopy to visualize other endovenous interventions, including radiofrequency ablation, glue ablation, and coil embolization. Other than applications described here, angioscopy has been used in management of venous thrombosis, assisting with thrombectomies and repair of deep venous valves. Angioscopy has been used for identification and management of acute thrombosis and has been reported to be superior to ultrasound-guided or venography-guided methods by which thrombus is only indirectly visualized.[1,13] In addition, it was pioneered by Gloviczki et al[32] in femoral vein valve repair under direct vision without venotomy.

Serious complications are rare but may include thrombosis secondary to intimal damage; extensive bruising after the procedure, especially if heparinized saline is used; potential for vessel wall puncture; infections; volume overload; and heart failure. Our patients did not experience any complications, recovered immediately, and had no evidence of bruising or clotting.

We followed the nonobstructive angioscopic principle of using the infusion of irrigation fluid to clear the visual field. Others have employed various methods[1,13] to obstruct the flow and to improve the visualization of the vessel lumen. Uchida[1] used a guiding catheter with a balloon at the tip through which the angioscope would protrude and the balloon would obstruct the flow distally, resulting in good outcomes. German researchers[13] used balloon catheters to occlude the vessel proximal to the tip of the angioscope. However, even after obstruction proximal and distal to the angioscopic tip, flow from tributaries draining into the visualized segment can still interfere with the field of view. This phasic tributary flow was observed in Video 7, *E* (online only).

Different types of irrigation fluids have been used in angioscopy to clear the field of vision, including dextran,[2,6,7] heparinized saline,[11] NS,[8,10] 5% dextrose,[14] and Ringer solution.[10,13] We used NS and could achieve reasonable results. The fluid was administered at a rate of 10 mL/min to a maximum of 750 mL in a 60-minute treatment session. Others have reported similar values. The group from Germany administered 350 to 500 mL of Ringer solution on average but also indicated that they occasionally used volumes >1000 mL when visualizing veins from time to time.[13] Warm saline is preferential to cold saline as cold saline has been reported to cause frost formation and to obscure the visual field as it comes in contact with warm blood (Video 6, *A*, online only). We were wary of using dextran, given the possibility of anaphylaxis or allergic reactions as well as the possibility of acute kidney injury.

The current angioscopic systems have multiple limitations. The requirement to clear the field of vision provides an extra step that other endoscopic procedures do not need. It can be a frustrating experience and only improves with time and technique, requiring a learning curve. The endovenous assessment with angioscopy is both qualitative and subjective. The interpretation of the visualized pathologic changes depends on the operator's experience, but given the real-time visualization of anatomic structures, the learning curve is not too steep and should be achievable for most endovascular specialists. The morphologic observations reported in this study need to be corroborated with histologic evaluation and other imaging modalities. Another limitation of angioscopy is the requirement for adjunctive modalities to determine the physical location of the angioscopic tip. Although the transilluminated tip can be visualized transcutaneously in the limbs, its visualization is greatly limited within the trunk. Our study was a pilot study to establish the application of this technique. Future studies should address the comparability of various venous imaging modalities, such as DUS, venography, and IVUS. We acknowledge that angioscopy potentially increases the cost of the procedure by adding an extra element. In our experience, this was helpful for the surgeon or interventionalist by providing direct real-time visualization of disease. Future studies should aim to quantitatively measure the difference in treatment outcome, occurrence of unnecessary intervention attempts, and complication rates with the use of angioscopy guidance.

CONCLUSIONS

Angioscopy offers many advantages over current imaging modalities in phlebology. It is a useful adjunct to the current armamentarium of investigative tools that phlebologists use. The technique and the instruments need improvement to facilitate a seamless and more straightforward procedure.

We acknowledge our nurses, Sabrina Melon and Antonia Graham, for useful suggestions to improve the saline irrigation; Dr Joseph Grace, for suggestions regarding patient positioning; Dr Martin Necas, for advice regarding hemodynamic observations; and Professor Lourens Bester and Dr Luke Baker, for assistance with interpretation of venographic images.

AUTHOR CONTRIBUTIONS

Conception and design: MK, KP
Analysis and interpretation: MK, AY, DC, KP
Data collection: MK, CH, TE, KP

Writing the article: MK, CH, TE, KP
Critical revision of the article: MK, AY, DC, KP
Final approval of the article: MK, CH, TE, AY, DC, KP
Statistical analysis: Not applicable
Obtained funding: Not applicable
Overall responsibility: KP

REFERENCES

1. Uchida Y. Recent advances in coronary angioscopy. J Cardiol 2011;57:18-30.
2. Komatsu S, Ohara T, Takahashi S, Takewa M, Minamiguchi H, Imai A, et al. Early detection of vulnerable atherosclerotic plaque for risk reduction of acute aortic rupture and thromboemboli and atheroemboli using non-obstructive angioscopy. Circ J 2015;79:742-50.
3. Kodama K, Asakura M, Ueda Y, Yamaguchi O, Hirayama A. The role of plaque rupture in the development of acute coronary syndrome evaluated by the coronary angioscope. Intern Med 2000;39:333-5.
4. Asakura M, Ueda Y, Yamaguchi O, Adachi T, Hirayama A, Hori M, et al. Extensive development of vulnerable plaques as a pan-coronary process in patients with myocardial infarction: an angioscopic study. J Am Coll Cardiol 2001;37:1284-8.
5. Hirayama A, Saito S, Ueda Y, Takayama T, Honye J, Komatsu S, et al. Qualitative and quantitative changes in coronary plaque associated with atorvastatin therapy. Circ J 2009;73:718-25.
6. Komatsu S, Hirayama A, Ueda Y, Okuyama Y, Ogasawara N, Kashiwase K, et al. Coronary ruptured plaque mimicking spontaneous coronary dissection in a young woman. Int J Cardiol 2006;113:288-9.
7. Komatsu S, Sato Y, Ueda Y, Achenbach S, Ebihara Y, Hirayama A, et al. Thrombotic occlusion proximal to plaque rupture in acute myocardial infarction: evaluation by intravascular ultrasound and coronary angioscopy. Int J Cardiol 2007;123:e12-4.
8. Gradman WS, Segalowitz J, Grundfest W. Venoscopy in varicose vein surgery: initial experience. Phlebology 1993;8:145-50.
9. Grundfest WS, Litvack F, Glick D, Segalowitz J, Treiman R, Cohen L, et al. Intraoperative decisions based on angioscopy in peripheral vascular surgery. Circulation 1988;78:I13-7.
10. Miller A, Campbell DR, Gibbons GW, Pomposelli FB Jr, Freeman DV, Jepsen SJ, et al. Routine intraoperative angioscopy in lower extremity revascularization. Arch Surg 1989;124:604-8.
11. Satokawa H, Hoshino S, Iwaya F, Igari T, Midorikawa H, Ogawa T. Intravascular imaging methods for venous disorders. Int J Angiol 2000;9:117-21.
12. Torsello G, Schwartz A, Aulich A, Sandmann W. Absorbable polydioxanone suture for venous anastomoses: experimental studies using venography and transluminal angioscopy. Eur J Vasc Surg 1987;1:319-25.
13. Woelfle KD, Bruijnen H, Zuegel N, Weber H, Jakob R, Loeprecht H. Technique and results of vascular endoscopy in arterial and venous reconstructions. Ann Vasc Surg 1992;6:347-56.
14. Biegeleisen K, Nielsen RD. Failure of angioscopically guided sclerotherapy to permanently obliterate greater saphenous varicosity. Phlebology 1994;9:21-4.
15. Radiation Safety Officer. Laser safety. Sydney, NSW: New South Wales Government Health; 2014.
16. Navarro L, Min RJ, Boné C. Endovenous laser: a new minimally invasive method of treatment for varicose veins—preliminary observations using an 810 nm diode laser. Dermatol Surg 2001;27:117-22.
17. Tessari L, Cavezzi A, Frullini A. Preliminary experience with a new sclerosing foam in the treatment of varicose veins. Dermatol Surg 2001;27:58-60.
18. Comerota AJ, Oostra C, Fayad Z, Gunning W, Henke P, Luke C, et al. A histological and functional description of the tissue causing chronic postthrombotic venous obstruction. Thromb Res 2015;135:882-7.
19. Labropoulos N, Patel PJ, Tiongson JE, Pryor L, Leon LR, Tassiopoulos AK. Patterns of venous reflux and obstruction in patients with skin damage due to chronic venous disease. Vasc Endovascular Surg 2007;41:33-40.
20. Mussa FF, Peden EK, Zhou W, Lin PH, Lumsden AB, Bush RL. Iliac vein stenting for chronic venous insufficiency. Tex Heart Inst J 2007;34:60-6.
21. Connor DE, Cooley-Andrade O, Goh WX, Ma DD, Parsi K. Detergent sclerosants are deactivated and consumed by circulating blood cells. Eur J Vasc Endovasc Surg 2015;49:426-31.
22. Parsi K. Interaction of detergent sclerosants with cell membranes. Phlebology 2015;30:306-15.
23. Parsi K, Exner T, Connor DE, Herbert A, Ma DD, Joseph JE. The lytic effects of detergent sclerosants on erythrocytes, platelets, endothelial cells and microparticles are attenuated by albumin and other plasma components in vitro. Eur J Vasc Endovasc Surg 2008;36:216-23.
24. Amzayyb M, van den Bos RR, Kodach VM, de Bruin DM, Nijsten T, Neumann HA, et al. Carbonized blood deposited on fibres during 810, 940 and 1,470 nm endovenous laser ablation: thickness and absorption by optical coherence tomography. Lasers Med Sci 2010;25:439-47.
25. Cameron E, Chen T, Connor DE, Behnia M, Parsi K. Sclerosant foam structure and stability is strongly influenced by liquid air fraction. Eur J Vasc Endovasc Surg 2013;46:488-94.
26. Wong K, Chen T, Connor DE, Behnia M, Parsi K. Basic physiochemical and rheological properties of detergent sclerosants. Phlebology 2015;30:339-49.
27. Wong KC, Chen T, Connor DE, Behnia M, Parsi K. Computational fluid dynamics of liquid and foam sclerosant injection in a vein model. Appl Mech Mater 2014;553:293-8.
28. Exner T, Rickard KA, Kronenberg H. Analysis of reptilase and thrombin-induced changes in fibrinogen subunits by isoelectric focussing. Thromb Res 1983;31:489-97.
29. State D. Use of human fibrin foam and thrombin solution as hemostatic agents in general surgery. Arch Surg 1949;58:284-90.
30. Arnoldussen CW, de Graaf R, Wittens CH, de Haan MW. Value of magnetic resonance venography and computed tomographic venography in lower extremity chronic venous disease. Phlebology 2013;28(Suppl 1):169-75.
31. Neglen P, Raju S. Intravascular ultrasound scan evaluation of the obstructed vein. J Vasc Surg 2002;35:694-700.
32. Gloviczki P, Merrell SW, Bower TC. Femoral vein valve repair under direct vision without venotomy: a modified technique with use of angioscopy. J Vasc Surg 1991;14:645-8.

Submitted Jan 15, 2019; accepted May 3, 2019.

Additional material for this article may be found online at www.jvsvenous.org.